Eur. J. Mineral.
2019, **31**, 1015–1024
Published online 27 July 2019

Hydroxylhedyphane, $Ca_2Pb_3(AsO_4)_3(OH)$, a new member of the apatite supergroup from Långban, Sweden

Cristian BIAGIONI[1,*], Ulf HÅLENIUS[2], Marco PASERO[1], Andreas KARLSSON[2] and Ferdinando BOSI[3,4]

[1]Dipartimento di Scienze della Terra, Università di Pisa, Via S. Maria 53, 56126 Pisa, Italy
*Corresponding author, e-mail: cristian.biagioni@unipi.it
[2]Department of Geosciences, Swedish Museum of Natural History, Box 50007, 10405 Stockholm, Sweden
[3]Dipartimento di Scienze della Terra, Sapienza Università di Roma, Piazzale Aldo Moro 5, 00185 Rome, Italy
[4]CNR, Istituto di Geologia Ambientale e Geoingegneria, U.O.S. di Roma, Roma, Italy

Abstract: The new mineral species hydroxylhedyphane, ideally $Ca_2Pb_3(AsO_4)_3(OH)$, has been discovered in the Långban Fe–Mn–(Ba–As–Pb–Sb) deposit, Filipstad district, Värmland, Sweden. It occurs as colourless prismatic crystals, up to 2.5 cm in length, forming an oriented intergrowth with a serpentine-subgroup mineral, as fracture-fillings cutting braunite and hausmannite ore. Electron-microprobe analysis yielded (mean of 16 spot analyses): P_2O_5 0.96(9), V_2O_5 0.07(4), As_2O_5 25.36(19), SiO_2 0.91(2), CaO 7.74(11), MnO 0.03(2), BaO 2.95(10), PbO 59.81(50), Na_2O 0.09(2), F 0.06(7), Cl 1.03(6), H_2O_{calc} 0.46, O = −(F + Cl) = –0.26, total 99.21. On the basis of 13 anions per formula unit, taking into account the crystal-structure data and the general formula of apatite-group minerals, the empirical formula of hydroxylhedyphane is $^{M(1)}(Ca_{1.56}Pb_{0.41}Mn_{0.01}Na_{0.03})_{\Sigma 2.01}$ $^{M(2)}(Pb_{2.80}Ba_{0.24}Ca_{0.09})_{\Sigma 3.13}$ $^{T}(As_{2.64}P_{0.16}V_{0.01}Si_{0.18})_{\Sigma 2.99}O_{12}$ $^{X}[(OH)_{0.61}Cl_{0.35}F_{0.04}]$. Main diffraction lines are [d(Å) (relative intensity) hkl]: 4.354 (21) 200; 4.138 (24) 111; 3.643 (33) 002; 3.291(31) 210; 2.999 (100) 211; 2.949 (41) 112; 2.903 (86) 300; and 2.177 (23) 400. Hydroxylhedyphane is trigonal, space group $P\bar{3}$, with a = 10.0414(3), c = 7.2752(2) Å, V = 635.28(4) Å^3, Z = 2. The crystal structure has been refined to R_1 = 0.034 on the basis of 1356 unique reflections with $F_o > 4\sigma(F_o)$ and 67 refined parameters. It agrees with the topology of the other apatite-supergroup minerals, with a symmetry reduction from $P6_3/m$ to $P\bar{3}$ and the splitting of the 4f M(1) site in the space group $P6_3/m$ into two distinct 2d sites M(1) and M(1)'. This lowering of symmetry is likely related to the preferential partitioning of Pb at the M(1) site. Finally, infrared spectroscopy suggests the possible occurrence of minor CO_2 in hydroxylhedyphane, but the crystal-structure refinement did not permit locating CO_3 groups.

Key-words: hydroxylhedyphane; apatite supergroup; calcium; lead; arsenic; arsenate; crystal structure; Långban; Sweden.

1. Introduction

Arsenate apatites are widely studied owing to their potential role in the sequestration and stabilization of As from polluted waters, an environmental problem affecting several areas world-wide, *e.g.*, in south-eastern Asia (*e.g.*, Charlet & Polya, 2006; Polya *et al.*, 2008). As suggested by Rakovan & Pasteris (2015), the accurate knowledge of the crystal chemistry of the arsenate apatites is thus crucial for environmental remediation. Up to now, seven arsenate apatite-supergroup minerals are known (Table 1), belonging to the apatite, hedyphane, and belovite groups. The crystal structure of these phases is known, the only exception being morelandite (Dunn & Rouse, 1978) for which data on the natural phase are not yet available. Usually these phases crystallize in the $P6_3/m$ space group, although a reduction to $P\bar{3}$ was observed in vanackerite (Schlüter *et al.*, 2016), owing to its peculiar chemical composition. Hydroxylhedyphane is a new addition to the arsenate apatite-supergroup minerals.

The first mention of what is likely hydroxylhedyphane was made by Sjögren (1891). He described a fibrous material from the Långban deposit, in Central Sweden, which the local miners called "asbest-hedyphan". During subsequent microscopic examination of the material he concluded that "asbest-hedyphan" consists of fine-scale intergrowths between a "hydrous magnesium-silicate" (*i.e.*, a serpentine-subgroup mineral) and a "lead-arsenate with traces of chlorine" (*i.e.*, a hedyphane-related mineral). Additionally, Dunn *et al.* (1985) described a "hydroxyl-bearing hedyphane" from Långban, Sweden, having OH^- as the dominant column anion. A fibrous material of similar character to hydroxylhedyphane was also reported, in samples from the same locality, by Hansen & O'Keeffe (1988) who described in detail its oriented intergrowth with a serpentine-subgroup mineral. On the basis of the finding of Dunn *et al.* (1985), Pasero *et al.* (2010) first introduced the name "hydroxylhedyphane".

The ores of the Långban mines were extracted for iron (primarily hematite and magnetite), and later manganese

0935-1221/19/0031-2878 $ 4.50
https://doi.org/10.1127/ejm/2019/0031-2878

Table 1. Chemical formula, unit-cell parameters, and space group (S.G.) of arsenate apatite-supergroup minerals.

Name	Chemical formula	*a* (Å)	*c* (Å)	*V* (Å^3)	S.G.	Ref.
Apatite group						
Johnbaumite	$Ca_5(AsO_4)_3OH$	9.72	6.97	570.3	$P6_3/m$	[1]
Mimetite	$Pb_5(AsO_4)_3Cl$	10.24	7.45	676.3	$P6_3/m$	[2]
Svabite	$Ca_5(AsO_4)_3F$	9.73	6.98	572.1	$P6_3/m$	[3]
Turneaureite	$Ca_5(AsO_4)_3Cl$	9.92	6.86	585.2	$P6_3/m$	[4]
Hedyphane group						
Hedyphane	$Ca_2Pb_3(AsO_4)_3Cl$	10.14	7.18	639.8	$P6_3/m$	[5]
Hydroxylhedyphane	$Ca_2Pb_3(AsO_4)_3OH$	10.04	7.28	635.3	$P\bar{3}$	[6]
Morelandite	$Ca_2Ba_3(AsO_4)_3Cl$	10.17	7.32	655.1	$P6_3$ or $P6_3/m$	[7]
Belovite group						
Vanackerite	$CdPbPb_3(AsO_4)Cl$	10.03	7.30	635.4	$P\bar{3}$	[8]

[1] Biagioni & Pasero (2013); [2] Okudera (2013); [3] Biagioni *et al.* (2016); [4] Biagioni *et al.* (2017); [5] Rouse *et al.* (1984); [6] this work; [7] Dunn & Rouse (1978); [8] Schlüter *et al.* (2016).

(in the form of braunite and hausmannite). During the last decades of mining operations, it was mined for carbonate (dolomite) (Magnusson, 1930; Holtstam & Langhof, 1999). The Långban deposit is hosted in Paleoproterozoic marbles and volcanogenic metasediments. The ores formed as chemical precipitates that reacted with hydrothermal solutions in an oxygen-rich, shallow submarine environment (Boström *et al.*, 1979). Subsequently, these rocks were affected by several episodes of metamorphic overprinting, which is manifested in complex, deformed ore bodies, skarn assemblages, and finally several generations of cavity and fissure mineralization. The deformed ore bodies and the recrystallized skarn assemblages are strongly altered by fluid-assisted metasomatism, which is in part responsible for the complex mineralogy found at Långban.

The exact timing of these events is not resolved but can in general terms be described as episodic metamorphic and metasomatic processes starting from emplacement at 1.9 Ga to the last metamorphic event at 1.0 Ga (Holtstam & Mansfeld, 2001). Textural observations suggest that hydroxylhedyphane may have crystallized during the later stages. The formation of hydroxylhedyphane probably occurred during stage "C" or "D" as described by Magnusson (1930). The late-stage paragenetic evolution of the fissure-hosted minerals has been further detailed by applying fluid-inclusion thermometry in Jonsson & Broman (2002).

This new mineral species (IMA 2018-052) and its name were approved by the Commission on New Minerals Nomenclature and Classification (CNMNC) of the International Mineralogical Association (IMA). The holotype specimen, catalogue number GEO-NRM#19070258, is deposited in the mineral collections at the Swedish Museum of Natural History in Stockholm, Sweden. The crystal used for single-crystal study is kept in the mineralogical collection at the Museo di Storia Naturale of the University of Pisa, Italy, under catalogue number #19897. The name is in agreement with its chemical composition, being the (OH)-dominant analogue of hedyphane, ideally $Ca_2Pb_3(AsO_4)_3Cl$ (Pasero *et al.*, 2010).

2. Occurrence and mineral description

2.1. Occurrence and physical properties

In the holotype specimen, hydroxylhedyphane occurs as colourless needles with a maximum crystal size (length) of about 25 mm, which are intergrown along $(10\bar{1}0)$ with a serpentine-subgroup mineral (Fig. 1). Hydroxylhedyphane and lamellae of a serpentine-subgroup mineral occur as fissure-fillings cutting dense braunite and hausmannite ore, which in turn is impregnated by calcite and barytocalcite (Fig 2a). Additionally, barytocalcite, fluorapatite and baryte may occur as irregular pods replacing hydroxylhedyphane and the serpentine-subgroup mineral, and are in some instances crosscutting the lamellae, which could be interpreted as a late replacement texture (Fig 2b). Sjögren (1891) mentioned that the sample of "asbest-hedyphane" he investigated was from "Bergråds sänkning" (a specific part of the Långban mine). It is likely that the holotype material comes from this shaft, but it cannot be excluded that it is from a different part of the mine.

Hydroxylhedyphane is colourless and transparent. It has a vitreous lustre and shows no cleavage or parting. The mineral is brittle and shows sub-conchoidal fractures. Due to intimate intergrowth with a serpentine-subgroup mineral (Fig. 2b), it was not possible to measure its density, but the calculated value, based on its empirical formula and single-crystal unit-cell parameters is 6.205 g cm^{-3}. In analogy with hedyphane, Mohs hardness of the mineral is estimated at 4–5.

The mineral is optically uniaxial negative, and it exhibits a low birefringence: $(\omega - \varepsilon) = 0.003$. The refractive indices were not measured, because the mean refractive index, 1.933, which was obtained from the Gladstone-Dale relationship (Mandarino, 1979, 1981) using the empirical formula, exceeds our experimental range due to safety regulations.

2.2. Chemical and spectroscopic data

Quantitative chemical analyses were obtained by electron-microprobe techniques (wavelength dispersive) using a

Fig. 1. Photograph of the holotype specimen. Hydroxylhedyphane in oriented intergrowth with a serpentine-subgroup mineral forming narrow lamellae. Width of photo is 31 mm. Sample GEO-NRM#19070258. Photo: Torbjörn Lorin.

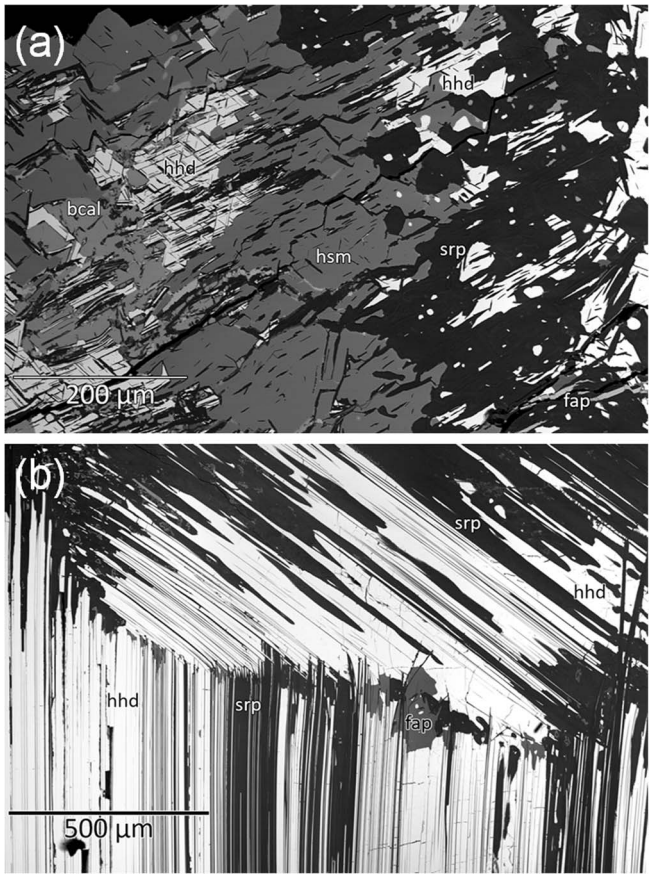

Fig. 2. Field-emission scanning electron microscope backscattered-electron (BSE) images of hydroxylhedyphane. In (a), this mineral is in contact with hausmannite, whereas in (b) hydroxylhedyphane and lamellae of a serpentine-subgroup mineral form an oriented intergrowth, with fluorapatite crosscutting these lamellae. Abbreviations: bcal, barytocalcite; fap, fluorapatite; hhd, hydroxylhedyphane; hsm, hausmannite; srp, serpentine-subgroup mineral. Sample GEO-NRM#19070258.

Cameca SX50 instrument (Istituto di Geologia Ambientale e Geoingegneria, CNR, Rome), operating at 15 kV, sample current of 15 nA, and with a beam diameter of 1 µm. Natural and synthetic standards (element, emission line) were: fluorapatite (P *K*α), baryte (S *K*α, Ba *L*α), jadeite (Na *K*α), orthoclase (K *K*α), vanadinite (V *K*α), sylvite (Cl *K*α), GaAs (As *L*α), galena (Pb *M*α), wollastonite (Si *K*α, Ca *K*α), celestine (Sr *L*α), rhodonite (Mn *K*α), magnetite (Fe *K*α), and fluorphlogopite (F *K*α). Sulphur, Fe, Sr, and K were below the detection limit. Because of intimate intergrowth between hydroxylhedyphane and a serpentine-subgroup mineral, direct determination of H_2O and CO_2 was not possible. The presence of hydroxyl groups is shown by Raman and infrared (IR) spectroscopy. The H_2O content was obtained by stoichiometry, on the basis of 13 anions and (OH + F + Cl) = 1.00 atom per formula unit (*apfu*), *i.e.*, in order to balance 25 positive charges. The IR spectra indicate the presence of minor CO_3 groups replacing AsO_4 groups. Chemical data are given in Table 2 (16 spot analyses). Neglecting minor CO_2, on the basis of 13 anions *pfu*, taking into account the crystal-structure data and the general formula of apatite-supergroup minerals, the empirical formula of hydroxylhedyphane is $^{M(1)}(Ca_{1.56}Pb_{0.41}Mn_{0.01}Na_{0.03})_{\Sigma 2.01}\ ^{M(2)}(Pb_{2.80}Ba_{0.24}Ca_{0.09})_{\Sigma 3.13}\ ^{T}(As_{2.64}P_{0.16}V_{0.01}Si_{0.18})_{\Sigma 2.99}O_{12}\ ^{X}[(OH)_{0.61}Cl_{0.35}F_{0.04}]$. The end-member formula of hydroxylhedyphane is $Ca_2Pb_3(AsO_4)_3(OH)$, corresponding to (in wt%) As_2O_5 30.36, CaO 9.88, PbO 58.97, H_2O 0.79, sum 100.00.

Unpolarized micro-Raman spectra were obtained on an unoriented sample of hydroxylhedyphane in nearly backscattered geometry with a Jobin-Yvon Horiba XploRA Plus apparatus (Dipartimento di Scienze della Terra, University of Pisa), equipped with a motorized *x*–*y* stage and an Olympus BX41 microscope with a 10× objective. The 532 nm line of a solid-state laser was used. The minimum lateral and depth resolution was set to a few µm. The system was calibrated using the 520.6 cm^{-1} Raman band of silicon before each experimental session. Spectra were collected through multiple acquisitions with single counting times of 30 s. Backscattered radiation was analysed with a 1200 mm^{-1} grating monochromator. Figure 3 shows the Raman spectrum of hydroxylhedyphane. In the region between 200 and 1200 cm^{-1} (Fig. 3a) the strongest bands are related to the stretching (bands at 772, 784, and 822 cm^{-1}) and bending modes of AsO_4 groups (326, 344, and 456 cm^{-1}), in agreement with the Raman spectrum of hedyphane reported by Frost *et al.* (2007). In the

Table 2. Electron-microprobe data for hydroxylhedyphane (mean of 16 spot analyses, in wt%).

Constituent	Mean	Range	e.s.d.
P_2O_5	0.96	0.82–1.10	0.09
V_2O_5	0.07	0.00–0.13	0.04
As_2O_5	25.36	24.94–25.63	0.19
SiO_2	0.91	0.89–0.95	0.02
CaO	7.74	7.58–7.95	0.11
MnO	0.03	0.00–0.07	0.02
BaO	2.95	2.75–3.13	0.10
PbO	59.81	59.14–61.00	0.50
Na_2O	0.09	0.04–0.12	0.02
F	0.06	0.00–0.19	0.07
Cl	1.03	0.91–1.19	0.06
H_2O_{calc}	0.46		
Sum	99.47		
O = F + Cl	–0.26		
Total	99.21		

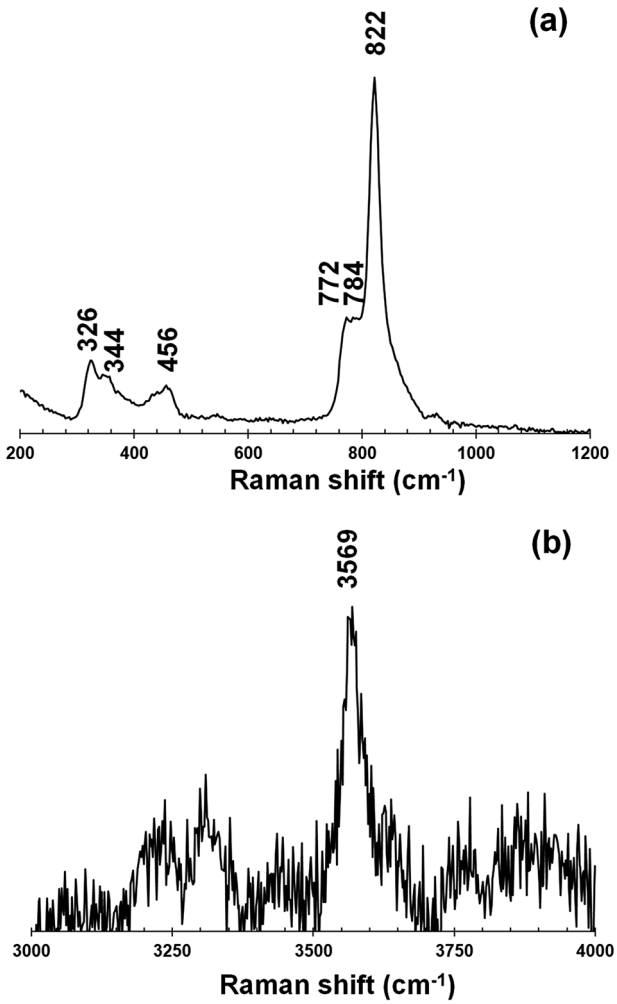

Fig. 3. Micro-Raman spectrum of hydroxylhedyphane, in the regions (a) 100–1200 cm^{-1} and (b) 3000–4000 cm^{-1}.

region between 3000 and 4000 cm^{-1} (Fig. 3b), the occurrence of a band at 3569 cm^{-1} confirms the presence of OH groups.

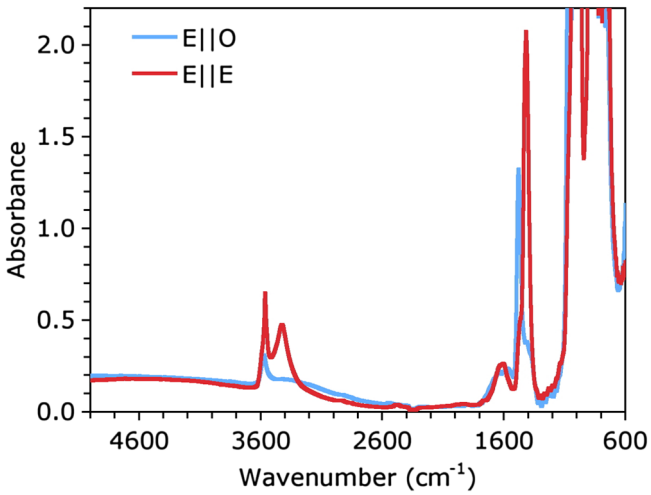

Fig. 4. Polarised single-crystal FTIR spectra of hydroxylhedyphane in the range 600–5000 cm^{-1}.

Polarized single-crystal IR spectra of hydroxylhedyphane (Fig. 4) were recorded with a Bruker Vertex 70 microscope spectrometer (Swedish Museum of Natural History, Stockholm) equipped with a halogen-lamp source, a KBr beam-splitter, a holographic ZnSe polarizer, and a midband MCT detector. The crystal was oriented by morphology and optical microscopy, and was doubly polished parallel to the **a**–**c** plane. The thickness of the single-crystal absorber was 49 μm. Polarized absorption spectra were acquired parallel (**E**||*E*) and perpendicular (**E**||*O*) to the **c**-axis over the wavenumber range 600–5000 cm^{-1} with a resolution of 2 cm^{-1} during 32 cycles. In order to ensure the absence of inclusions of other minerals, the measuring aperture was decreased to 60 × 60 μm. The recorded spectra show absorption bands due to OH-stretching modes in the range 3400–3600 cm^{-1}, bands related to vibrations in CO_3 groups in the range 1400–1500 cm^{-1} and very strong absorption below 1100 cm^{-1} due to fundamental modes in AsO_4 and PO_4 groups. The bands at 1410 and 1475 cm^{-1} are caused by ν_3-modes in CO_3 groups that replace TO_4 groups in the apatite structure (Fleet *et al.*, 2004). Hydroxyl-stretching bands occur at 3425, 3550, 3565, and 3575 cm^{-1}. With the exception of the band at 3575 cm^{-1} all these bands are strongly polarized in **E**||*E*. The latter band and a band at ~1600 cm^{-1} are tentatively assigned to H_2O groups. None of the bands in the range 3600–3700 cm^{-1} that are related to OH-stretching in serpentine-subgroup minerals were observed. Using the IR method for quantification of OH in apatite (Wang *et al.*, 2011), the H_2O content in the hydroxylhedyphane specimen is calculated to be at ~0.2 wt%, which is lower than the water concentration of 0.46 wt% calculated for the empirical formula on the basis of electron-microprobe analysis. Application of the calibration for water contents in apatite to structurally related arsenates generally seems to result in estimates that are too low by a factor of 2 (Biagioni *et al.*, 2016, 2017). Based on a linear absorption coefficient of 200–400 L mol^{-1} cm^{-1} for the ν_3-bands of CO_3 groups in spectra of a wide range of glasses (von Aulock *et al.*, 2014), the CO_2 concentration

in the hydroxylhedyphane is calculated to be in the range 0.27–0.55 wt%. The possible incorporation of CO_3 groups in the crystal structure of hydroxylhedyphane is discussed below.

2.3. X-ray crystallography and structure refinement

Powder X-ray diffraction data were collected on a PANalytical X'Pert^3 Powder diffractometer (Swedish Museum of Natural History, Stockholm) fitted with an X'celerator silicon-strip detector and operated at 40 mA and 45 kV (Cu $K\alpha$ radiation, λ = 1.5406 Å). Peak positions were determined with the HighScore Plus 4.6 software and corrected against an external Si standard (NIST SRM640). Prior to powder X-ray data collection, optically homogenous pieces of hydroxylhedyphane were powdered in an agate mortar and then processed with MI (methylene iodide, ρ = 3200 kg m^{-3}) in order to remove the serpentine-subgroup mineral. This process was repeated twice. Indexed d values and background-subtracted relative peak-heights are given in Table 3. The trigonal unit-cell parameters, obtained by least-squares refinement of 38 reflections, are a = 10.050(1), c = 7.278(2) Å and V = 636.64(3) Å^3.

After chemical analysis, the same crystal was removed from the epoxy and used for X-ray diffraction measurements on a Bruker KAPPA APEX-II single-crystal diffractometer (Sapienza University of Rome) equipped with a CCD area detector (6.2 × 6.2 cm^2 active detection area, 512 × 512 pixels) and a graphite crystal monochromator, using Mo$K\alpha$ radiation from a fine-focus sealed X-ray tube. The sample-to-detector distance was 4 cm. The measurement returned the following unit-cell parameters: a = 10.0414(3), c = 7.2752(2) Å, V = 635.28(4) Å^3, with the c:a ratio = 0.7245.

A total of 2166 exposures (step = 0.3°, time/step = 20 s) covering a full reciprocal sphere, with a redundancy of about 7, were collected using ω and φ scan modes. Intensity data were integrated and corrected for Lorentz, polarization, background and absorption using the package of software *Apex*2 (Bruker AXS Inc., 2004). The statistical tests on the distribution of $|E|$ values ($|E^2 - 1|$ = 0.934) indicated the presence of an inversion centre. The systematic-absence analyses strongly suggested the choice of the space group $P\bar{3}$. The crystal structure was refined using *Shelxl*-2018 (Sheldrick, 2015) starting from the atomic coordinates of belovite-(La) from Kabalov *et al.* (1997). The following neutral scattering curves, from the *International Tables for Crystallography* (Wilson, 1992), were initially used: Ca *vs.* Pb at the M(1), M(1)', and M(2) sites, and As *vs.* Si at the T site. An isotropic refinement converged to R_1 = 10.2%, confirming the correctness of the structural model. In order to avoid high correlation values, the site occupancies at the T, X(1), and X(2) sites were fixed on the basis of electron-microprobe data. Between X(1) and X(2), Cl was preferentially located at the X(1) site, which shows the highest site scattering and the longest distance from cation sites. Assuming anisotropic displacement parameters for cations, the R_1 converged to 5.6%, which was further lowered to 5.0% using an anisotropic model for all atom positions but the X(1) and X(2) sites. Finally, the occurrence of a twin axis parallel to [0001], likely related to the symmetry reduction of the apatite structure type (space group $P6_3/m$) to $P\bar{3}$, was taken into account. The final refinement converged to R_1 = 3.4% for 1356 unique reflections with $F_o > 4\sigma(F_o)$ and 67 refined parameters. Details of the selected crystal, data collection, and refinement are given in Table 4. Fractional atomic coordinates and isotropic or equivalent isotropic parameters are reported in Table 5, whereas Table 6 reports selected bond distances. Table 7 shows the comparison between observed and calculated site

Table 3. Powder X-ray diffraction data (d in Å) for hydroxylhedyphane.

d_{obs}	I_{obs}	*d_{calc}	**I_{calc}	**d_{calc}	h	k	l
8.717	11	8.704	4	8.696	1	0	0
–	–	–	2	5.580	1	0	1
5.030	12	5.025	5	5.021	1	1	0
4.354	21	4.352	8	4.348	2	0	0
4.138	24	4.135	31	4.132	1	1	1
3.737	3	3.735	2	3.732	2	0	1
3.643	33	3.639	23	3.638	0	0	2
3.358	10	3.357	9	3.356	1	0	2
3.291	31	3.290	17	3.287	2	1	0
2.999	100	2.998	100	2.995	2	1	1
2.949	41	2.947	41	2.946	1	1	2
2.903	86	2.901	26	2.899	3	0	0
2.695	1	2.695	1	2.693	3	0	1
2.441	4	2.440	6	2.439	2	1	2
–	–	–	3	2.412	3	1	0
2.292	3	2.291	3	2.289	3	1	1
2.186	6	2.185	11	2.184	1	1	3
2.177	23	2.176	9	2.174	4	0	0
2.068	9	2.068	16	2.066	2	2	2
2.012	5	2.012	8	2.010	3	1	2
1.997	4	1.997	4	1.995	3	2	0
1.953	19	1.952	31	1.951	2	1	3
1.926	14	1.926	23	1.924	3	2	1
1.900	11	1.899	8	1.898	4	1	0
1.868	12	1.868	21	1.866	4	0	2
1.819	5	1.819	9	1.819	0	0	4
–	–	1.741	1	1.749	3	2	2
1.741	3	–	1	1.739	5	0	0
1.711	1	1.711	2	1.710	3	1	3
–	–	–	1	1.678	2	0	4
1.645	4	1.645	4	1.643	4	2	0
1.632	4	1.632	8	1.631	3	3	1
–	–	–	1	1.603	4	2	1
1.593	2	1.592	5	1.591	2	1	4
1.570	3	1.570	5	1.569	5	0	2
1.563	3	1.563	3	1.562	5	1	0
1.541	6	1.541	17	1.541	3	0	4
1.528	7	1.528	12	1.527	5	1	1
–	–	–	4	1.520	3	3	2
1.499	1	1.499	4	1.498	4	2	2
1.430	1	1.431	2	1.435	4	3	0
–	–	1.396	2	1.398	1	1	5
1.395	1	–	5	1.395	4	0	4
1.378	1	1.378	4	1.377	3	3	3
1.369	2	1.369	6	1.368	5	2	1

*Calculated from unit-cell refinement from X-ray powder data.
**Calculated from single-crystal structural model. Only reflections with $I > 1$ are listed.

Table 4. Crystal data and summary of parameters describing data collection and refinement for hydroxylhedyphane.

Crystal data	
Crystal size (mm)	0.20 × 0.20 × 0.25
Cell setting, space group	Trigonal, $P\bar{3}$
a (Å)	10.0414(3)
c (Å)	7.2752(2)
V (Å^3)	635.28(4)
Z	2
Data collection and refinement	
Radiation, wavelength (Å)	Mo$K\alpha$, 0.71073
Temperature (K)	293
$2\theta_{max}$ (°)	64.18
Measured reflections	10 524
Unique reflections	1454
Reflections with $F_o > 4\sigma(F_o)$	1356
R_{int}	0.0672
$R\sigma$	0.0343
Range of h, k, l	$-15 \le h \le 14$, $-15 \le k \le 14$, $-10 \le l \le 9$
R [$F_o > 4\sigma(F_o)$]	0.0342
R (all data)	0.0372
wR (on F_o^2)	0.0793
Goof	1.059
Least-squares parameters	67
Maximum and minimum residual peak (e Å^{-3})	3.73 [at 0.70 Å from M(2)] −3.65 [at 0.64 Å from M(2)]

scattering; the latter are based on the proposed site population. Table 8 gives the weighted bond-valence sums obtained from the bond-valence parameters of Brese & O'Keeffe (1991) for all cation–anion pair except for the Pb–O pair from Krivovichev (2012).

3. Crystal-structure description

The crystal structure of hydroxylhedyphane (Fig. 5) is topologically identical to those of the other apatite supergroup minerals (Pasero *et al.*, 2010). However, a symmetry reduction from the space group $P6_3/m$ to $P\bar{3}$ occurs as a consequence of the splitting of the 4*f* site in $P6_3/m$ into two distinct 2*d* sites of $P\bar{3}$. Indeed, the M(1) site of hedyphane is split into two distinct sites, otherwise related by a (0, 0, ½) shift in the $P6_3/m$ space group. One of these two sites [labelled as M(1)'] is almost exclusively occupied by Ca, whereas the other [labelled as M(1)] has a site population close to ($Ca_{0.6}Pb_{0.4}$). Most likely the preferential partitioning of Pb at the M(1) site induces the lowering of symmetry from hexagonal to trigonal.

The M(1) and M(1)' sites are nine-fold coordinated and can be described as tricapped trigonal prisms. These polyhedra share {0001} pinacoid faces forming chains running along **c** (Fig. 5). The M(1) site has an average bond distance of 2.66 Å, with three shorter distances at 2.44 Å and six longer ones, in the range 2.76–2.78 Å. In contrast, M(1)' has six short bonds in the range 2.40–2.45 Å, and three longer (= weaker) bonds at 3.07 Å. The average <M(1)'–O> distance is 2.64 Å. In hedyphane (Rouse *et al.*, 1984), the M(1) site has six bonds in the range 2.38–2.55 Å and three longer bonds at 2.86 Å, with an average <M(1)–O> distance of 2.60 Å. Refined site scattering values at the M(1) and M(1)' sites are consistent with a mixed (Ca,Pb) and a pure Ca site population, respectively (Table 7).

Adjacent M(1) + M(1)' columns are connected by TO_4 tetrahedra through corner-sharing. Average <T–O> distance is 1.66 Å, shorter than the value observed in hedyphane (1.69 Å), owing to the minor substitution of As^{5+} by P^{5+} and Si^{4+}.

Within the framework formed by M(1) + M(1)' columns and TO_4 tetrahedra, the M(2) polyhedra are hosted. In hydroxylhedyphane, the M(2) site is eight-fold coordinated, with five bond distances in the range 2.40–2.82 Å and three additional ones between 3.09 and 3.17 Å. In agreement with the refined site scattering, the M(2) site hosts Pb, and minor Ba and Ca.

Neglecting the very low F content (0.04 *apfu*), the studied specimen is in the binary system between hedyphane, ideally $Ca_2Pb_3(AsO_4)_3Cl$, and hydroxylhedyphane, ideally $Ca_2Pb_3(AsO_4)_3(OH)$, containing *ca.* 35 mol% of hedyphane. In the latter phase, Rouse *et al.* (1984) located the column anions at the position (0, 0, 0). Previous studies (*e.g.*, Hughes *et al.*, 1989) demonstrated that the anion positions in binary and ternary apatite systems cannot be predicted from their coordinates in the end-members. As a consequence of the symmetry reduction from $P6_3/m$ to $P\bar{3}$, the anion site at (0, 0, 0) (Wyckoff position 2*b*) in hedyphane corresponds to the two independent 1*a* and 1*b* sites in hydroxylhedyphane. Taking into account the observed site scattering and the M(2)–X distances, minor Cl was located

Table 5. Structural sites, Wyckoff positions, site occupation factors (s.o.f.), fractional atomic coordinates, and isotropic (*) or equivalent isotropic displacement parameters (in Å^2) for hydroxylhedyphane. U_{eq} is defined as one third of the trace of the orthogonalized U_{ij} tensor.

Site	Wyckoff position	s.o.f.	x	y	z	$U_{eq/iso}$
M(1)	2*d*	$Ca_{0.57(1)}Pb_{0.43(1)}$	1/3	2/3	0.01032(15)	0.0129(3)
M(1)'	2*d*	$Ca_{0.95(1)}Pb_{0.05(1)}$	1/3	2/3	0.4898(4)	0.0158(8)
M(2)	6*g*	$Pb_{0.92(1)}Ca_{0.08(1)}$	0.25417(4)	0.00368(4)	0.25561(7)	0.02220(13)
T	6*g*	$As_{0.88}Si_{0.06}P_{0.05}V_{0.01}$	0.41200(8)	0.38413(8)	0.25242(13)	0.0090(2)
O(1)	6*g*	$O_{1.00}$	0.5077(7)	0.1586(6)	0.7464(11)	0.0209(12)
O(2)	6*g*	$O_{1.00}$	0.3748(13)	0.2826(12)	0.0600(12)	0.040(2)
O(3)	6*g*	$O_{1.00}$	0.3365(16)	0.2568(11)	0.4224(14)	0.054(3)
O(4)	6*g*	$O_{1.00}$	0.5285(8)	0.1310(8)	0.2813(16)	0.039(2)
X(1)	1*a*	$Cl_{0.70}(OH)_{0.30}$	0	0	0	0.048(2)*
X(2)	1*b*	$(OH)_{1.00}$	0	0	½	0.048(2)*

Table 6. Selected bond distances (in Å) for hydroxylhedyphane.

M(1)	–O(1)	2.441(7) × 3	*M*(1)'	–O(1)	2.404(7) × 3
	–O(4)	2.760(10) × 3		–O(4)	2.451(9) × 3
	–O(2)	2.781(11) × 3		–O(3)	3.073(14) × 3
M(2)	–O(4)	2.395(7)	*T*	–O(1)	1.650(6)
	–O(3)	2.492(9)		–O(2)	1.660(8)
	–O(3)	2.553(10)		–O(3)	1.664(8)
	–O(2)	2.561(8)		–O(4)	1.672(7)
	–O(2)	2.819(11)			
	–*X*(2)	3.0955(4)			
	–*X*(1)	3.1431(4)			
	–O(1)	3.173(7)			

Table 7. Refined site scattering *vs.* calculated site scattering (in electrons) and site population at the *M* sites for hydroxylhedyphane.

Site	Refined scattering	Proposed population	Calculated scattering
M(1)	46.7	$Ca_{0.57}Pb_{0.43}$	46.7
M(1)'	23.1	$Ca_{0.95}Pb_{0.05}$	23.1
M(2)	77.0	$Pb_{0.88}Ba_{0.08}Ca_{0.04}$	77.4

at the former position, labelled as *X*(1), forming a (relatively) longer bond distance with *M*(2). On the contrary, *X*(2) is interpreted as a pure (OH) site. It is worth noting that in calcium apatites hydroxyl groups are usually displaced from the mirror plane, being disordered 0.35 Å above or below the (0, 0, ¼) position (*e.g.*, Hughes *et al.*, 1989; Biagioni & Pasero, 2013). However, no evidence of such a displacement was observed in hydroxylhedyphane, where OH groups seem to be located at positions lying on the mirror plane (as, for instance, in turneaureite – Biagioni *et al.*, 2017).

4. Discussion

4.1. Hydroxylhedyphane in the framework of the hedyphane group

The chemistry of the studied specimen of hydroxylhedyphane matches the previous description given by Dunn *et al.* (1985), who reported the presence of Ba as a characteristic feature of hedyphane-group minerals from Långban and a Pb:Ca atomic ratio higher than 3:2, with Pb > 3 *apfu* and Ca < 1.7 *apfu*. Finally, the Si^{4+} content was confirmed.

Hydroxylhedyphane is the second hedyphane-group species containing OH as the dominant column anion, the other one being cesanite, $Ca_2Na_3(SO_4)_3(OH)$ (Cavarretta *et al.*, 1981; Tazzoli, 1983; Piotrowski *et al.*, 2002).

White & Dong (2003) gave a compilation of 77 distinct apatite compounds for which complete crystallographic data are available. Among them, only 9% is represented by $P\bar{3}$ apatites. Hydroxylhedyphane is a further addition to this group, being one of the few natural species belonging to the apatite supergroup showing this trigonal space-group symmetry, along with some members of the belovite group, *i.e.*, belovite-(Ce), belovite-(La), carlgieseckeite-(Nd), kuannersuite-(Ce), and vanackerite. Moreover, the studied sample suggests the hypothetical existence of $CaPbPb_3(AsO_4)_3(OH)$, the Ca–(OH) analogue of vanackerite, $CdPbPb_3(AsO_4)_3Cl$ (Schlüter *et al.*, 2016). Following Pasero *et al.* (2010), this should be an arsenate member of the belovite group, a series of hexagonal and trigonal apatite-group minerals with the *M*(1) site split into the *M*(1) and *M*(1)' sites containing different dominant (*i.e.*, species-defining) cations. Hydroxylhedyphane shows the splitting of *M*(1) site of $P6_3/m$ apatite into *M*(1) and *M*(1)', owing to the symmetry reduction. However, both sites have the same dominant cation, Ca^{2+}. Consequently, it can be considered a member of the hedyphane group, but it also suggests the possibility of intermediate phases between the hedyphane and belovite groups.

The unit-cell volume of hydroxylhedyphane is only slightly smaller than that of hedyphane (635.3 *vs.* 639.8 $Å^3$, respectively; $\Delta V = -0.7\%$), notwithstanding the smaller size of OH group with respect to the Cl anion. Likely, the contraction induced by the Cl → OH substitution is partially balanced by the $Ca^{2+} \rightarrow Pb^{2+}$ substitution at the *M*(1) + *M*(1)' sites. As observed by Biagioni *et al.* (2017) for the calcium arsenate apatites, the Cl → OH substitution induces a contraction of the *a*-parameter ($\Delta a = -0.1\%$) and an expansion of the *c*-parameter ($\Delta c = +1.4\%$).

Taking into account the symmetry reduction and the different dominant anions at *X*(1) and *X*(2), the chemical formula of the studied sample could be written as $Ca_4Pb_6(AsO_4)_6(OH)Cl$ (Z = 1). Two species belonging to the belovite group are characterized by a similar anion ordering, *i.e.*, deloneite and kuannersuite-(Ce) (Pasero *et al.*, 2010). Friis *et al.* (2004) discussed the ordering of F and Cl in

Table 8. Weighted bond-valence balance (in valence units) for hydroxylhedyphane.

Site	O(1)	O(2)	O(3)	O(4)	*X*(1)	*X*(2)	Σ cations
M(1)	$^{3\times\rightarrow}0.32$	$^{3\times\rightarrow}0.14$		$^{3\times\rightarrow}0.15$			1.83
M(1)'	$^{3\times\rightarrow}0.31$		$^{3\times\rightarrow}0.05$	$^{3\times\rightarrow}0.28$			1.92
M(2)	0.02	0.31	0.35	0.44	$0.08^{\times6\downarrow}$	$0.10^{\times6\downarrow}$	1.79
		0.18	0.31				
T	1.32	1.29	1.27	1.25			5.13
Σ anions	1.97	1.92	1.98	2.12	0.48	0.60	

Note. Left and right superscripts indicate the number of equivalent bonds involving cations and anions, respectively. For sites with mixed occupancy, the bond valences have been weighted according to the empirical formula and Table 7.

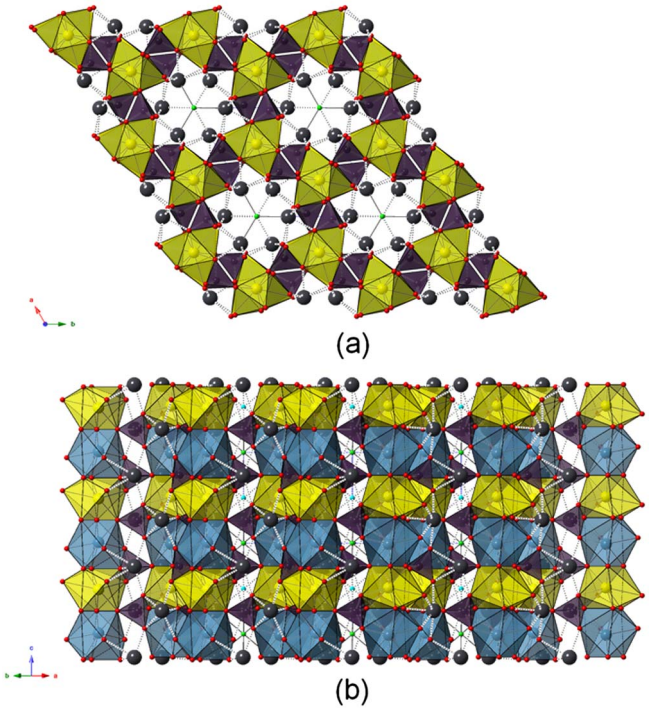

Fig. 5. Crystal structure of hydroxylhedyphane as seen down [0001] (a) and [11$\bar{2}$0] (b). Symbols: light blue polyhedra = *M*(1) site; yellow polyhedra = *M*(1)' site; violet polyhedra = *T* site. Circles: grey = *M*(2) site; green = *X*(1) site; light blue = *X*(2) site.

kuannersuite-(Ce), pointing out that such an ordered distribution is connected with the occupancy of the tricapped trigonal prisms and the tilting of the subvertical edge of the (PO_4) groups. Similarly, the tilting of the O(2)–O(3) edge of the (AsO_4) group in the studied hydroxylhedyphane seems to be related to the anion ordering. Indeed, Cl is located at the *X*(1) site, at the same level of the (Ca,Pb)-hosting *M*(1) site; the oxygen atoms hosted at O(2), which are the capping atoms of *M*(1), are shifted closer to the central atom and farther away from the *X*(1) site, thus favouring the hosting of the large anion Cl. At the same time, O(3), the capping ligand of the almost Ca pure *M*(1)' site, is moved away from the central atom and closer to the *X*(2) position, where the smaller (OH) group occurs. This anion ordering is an interesting crystal-chemical feature. However, for nomenclature purposes, the *X*(1) and *X*(2) sites should be considered as an aggregate site, in keeping with the formulae of other hedyphane-group minerals. The end-member formula of hydroxylhedyphane is indeed $Ca_2Pb_3(AsO_4)_3(OH)$ (*Z* = 2).

4.2. Carbonate groups in hydroxylhedyphane

The occurrence of minor CO_3 groups in natural apatites was reported by previous authors. For instance, Sänger & Kuhs (1992) reported the presence of very weak absorption bands in the IR spectrum of hydroxylapatite, intimately intergrown with chrysotile, from the Totenkopf area, Stubachtal, Austria. They related these bands to $(CO_3)^{2-}$ ions in two different structural positions.

The two different ways for hosting carbonate groups in the apatite structure are indicated as type A, when CO_3 occurs in the anion columns (further subdivided in type A1 and A2, according to the CO_3 configuration), and as type B, when it substitutes the tetrahedrally coordinated ions (*e.g.*, Fleet *et al.*, 2004; Wilson *et al.*, 2004). The positions of the bands observed in the IR spectra of hydroxylhedyphane (*i.e.*, 1410 and 1475 cm^{-1}) agree with the ν_3 bands at ~1406 and ~1470 cm^{-1} reported by Fleet *et al.* (2004) for type B CO_3 groups. There is no evidence for the occurrence of type-A CO_3 groups.

The replacement of $(AsO_4)^{3-}$ by $(CO_3)^{2-}$ could be balanced according to different mechanisms. In agreement with LeGeros *et al.* (1968), a possible substitution mechanism could be $Ca^{2+} + (TO_4)^{3-} \rightarrow Na^{+} + (CO_3)^{2-}$, where *T* = As in hydroxylhedyphane. However, the Na content in the studied sample is very low (0.03 *apfu*) and cannot explain the observed amount of $(CO_3)^{2-}$, ranging between 0.07 and 0.14 CO_3 groups *pfu*, representing the minimum and maximum estimates, respectively. Other authors proposed the occurrence of vacancies at $^{M(1,2)}$Ca and (OH) sites according to the stoichiometry $Ca_{10-x}Na_{2x/3}(TO_4)_{6-x}(CO_3)_x(H_2O)_x(OH)_{2-x/3}$ (*e.g.*, Bonel *et al.*, 1975; Ivanova *et al.*, 2001). Although infrared spectroscopy of hydroxylhedyphane indicated the occurrence of a band, tentatively attributed to the bending of O–H bonds in H_2O groups, no detectable vacancies at the *M*(1,2) sites are suggested by the refined site-scattering values. Another mechanism was proposed by Yi *et al.* (2013): the $(CO_3)^{2-}$ group could lie on the sloping face of a $(TO_4)^{3-}$ tetrahedron, with an F anion located at the remaining vertex. However, the studied hydroxylhedyphane contains only a very low amount of F (0.04 *apfu*), which does not support this model. Moreover, the refinement of the site occupation factor (s.o.f.) at the *T* site using the scattering curves of As *vs.* Si did not result in a significant discrepancy between observed and calculated site scattering, *i.e.*, 30.5 and 30.7 electrons per formula unit, respectively. Likely, the low amount of $(CO_3)^{2-}$ groups did not significantly affect the crystal-structure refinement, contrary to what was reported by other authors (*e.g.*, Cámara *et al.*, 2018).

Hydroxylhedyphane is characterized by detectable amounts of Si. Usually, the occurrence of $(SiO_4)^{4-}$ in apatite-supergroup minerals is coupled with the occurrence of either trivalent cations at *M* sites, as observed in the britholite group, or with the occurrence of $(SO_4)^{2-}$, as in the ellestadite group. However, in the studied sample, no evidence for the occurrence of REE^{3+} or $(SO_4)^{2-}$ was observed. Consequently, the substitution $2(AsO_4)^{3-} = (CO_3)^{2-} + (SiO_4)^{4-}$ could be another possible mechanism. Taking into account the highest possible CO_2 content suggested by Fourier-transform IR spectroscopy (*i.e.*, 0.55 wt%), the following crystal-chemical formula, obtained on the basis of (As + P + V + Si + C) = 3 *apfu*, may be written (with rounding errors): $^{M(1)}(Ca_{1.58}Pb_{0.29}Na_{0.03})_{\Sigma 1.90}$ $^{M(2)}(Pb_{2.78}Ba_{0.22})_{\Sigma 3.00}$ $^{T}[(As_{2.52}P_{0.15}V_{0.01}Si_{0.17})_{\Sigma 2.85}O_{11.32}](CO_3)_{0.14}$ $^{X}[(OH)_{0.63}Cl_{0.33}F_{0.04}]$. By using the lowest CO_2 estimate (0.27 wt%), the formula $^{M(1)}(Ca_{1.62}Pb_{0.37}Na_{0.03})_{\Sigma 2.02}$

$^{M(2)}(Pb_{2.77}Ba_{0.23})_{\Sigma 3.00}$ $^{T}[(As_{2.58}P_{0.16}V_{0.01}Si_{0.18})_{\Sigma 2.93}O_{11.68}]$ $(CO_3)_{0.07}$ $^{X}[(OH)_{0.60}Cl_{0.34}F_{0.04}]$ can be obtained.

Another possible hypothesis explaining the presence of CO_3 groups takes into account the substitution mechanism $[^{A2}(CO_3)^{2-} + 2^{B}(CO_3)^{2-} = {}^{A2}\square + 2(AsO_4)^{3-}]$, in agreement with Fleet *et al.* (2004). Since the total CO_2 content in the studied sample is less than 0.55 wt%, it is reasonable to hypothesize that the $^{A2}CO_3$ should be very low, close to 0.05 CO_3 per formula unit, not allowing its detection through IR spectroscopy. This is in agreement with the observation that the entry of moderate amounts of $^{A2}CO_3$ is usually a high-pressure feature, and consequently the CO_3-to-AsO_4 substitution should involve other charge-compensation mechanisms. However, minor CO_3 groups in the anion columns have to be related to the substitution $2(OH)^- = (CO_3)^{2-} + \square$. Consequently, the chemical formula of the studied sample, assuming this second hypothesis and the highest CO_2 estimate, may be rewritten as (with rounding errors) $^{M(1)}(Ca_{1.61}Pb_{0.35}Na_{0.03})_{\Sigma 1.99}$ $^{M(2)}(Pb_{2.78}Ba_{0.22})_{\Sigma 2.99}$ $^{T}(As_{2.58}P_{0.16}V_{0.01}Si_{0.18})_{\Sigma 2.93}$ $O_{11.59}$ $(CO_3)_{0.10}$ $[(OH)_{0.53}Cl_{0.34}(CO_3)_{0.05}F_{0.04}]_{\Sigma 0.96}$.

Admittedly, the incorporation of carbonate groups within the apatite framework is a long-time puzzle. Our refinement of the crystal structure of hydroxylhedyphane did not allow locating the occurrence of CO_3 groups. Indeed, as noted by Fleet *et al.* (2004), the combination of partial occupancy and disorder of CO_3 groups results in these groups being represented by features considerably weaker than a hydrogen atom. As a matter of fact, the relatively large U_{eq} values shown by three O atoms at the O(2), O(3), and O(4) sites may be at least partially explained by some kind of rotational disorder of AsO_4 groups due to the carbonate-for-arsenate substitution, in addition to the Cl-to-OH substitution and the twinned nature of the studied crystal.

Acknowledgements: CB acknowledges financial support from the University of Pisa through the project P.R.A. 2018–2019 "Georisorse e Ambiente" (Grant No. PRA_2018_41). We thank T. Lorin for the colour photograph of the holotype specimen. We wish to thank the Associate Editor E.S. Grew, I. Pekov, and an anonymous reviewer for their constructive criticisms.

References

Biagioni, C. & Pasero, M. (2013): The crystal structure of johnbaumite, $Ca_5(AsO_4)_3OH$, the arsenate analogue of hydroxylapatite. *Am. Mineral.*, **98**, 1580–1584.

Biagioni, C., Bosi, F., Hålenius, U., Pasero, M. (2016): The crystal structure of svabite, $Ca_5(AsO_4)_3F$, an arsenate member of the apatite supergroup. *Am. Mineral.*, **101**, 1750–1755.

—, —, —, — (2017): The crystal structure of turneaureite, $Ca_5(AsO_4)_3Cl$, the arsenate analog of chlorapatite, and its relationships with the arsenate apatites johnbaumite and svabite. *Am. Mineral.*, **102**, 1981–1986.

Bonel, G., Labarthe, J.C., Vignoles, C. (1975): Contribution à l'étude structurale des apatites carbonatées de type B. *in* "Physico-Chimie et Cristallographie des Apatites d'Intérêt Biologique, Colloques Internationaux du Centre National de la Recherche Scientifique No. 230, 1973". CNRS, Paris, 117–125.

Boström, K., Rydell, H., Joensuu, O. (1979): Langban; an exhalative sedimentary deposit? *Econ. Geol.*, **74**, 1002–1011.

Brese, N.E. & O'Keeffe, M. (1991): Bond-valence parameters for solids. *Acta Crystallogr.*, **B47**, 192–197.

Bruker AXS Inc. (2004): APEX 2. Bruker Advanced X-ray Solutions, Madison, WI, USA.

Cámara, F., Curetti, N., Benna, P., Abdu, Y.A., Hawthorne, F.C., Ferraris, C. (2018): The effect of type-B carbonate content on the elasticity of fluorapatite. *Phys. Chem. Minerals*, **45**, 789–800.

Cavarretta, G., Mottana, A., Tecce, F. (1981): Cesanite, $Ca_2Na_3[(OH)(SO_4)_3]$, a sulphate isotypic to apatite, from the Cesano geothermal field (Latium, Italy). *Mineral. Mag.*, **44**, 269–273.

Charlet, L. & Polya, D.A. (2006): Arsenic in shallow, reducing groundwaters in Southern Asia: an environmental health disaster. *Elements*, **2**, 91–96.

Dunn, P.J. & Rouse, R.C. (1978): Morelandite, a new barium arsenate chloride member of the apatite group. *Can. Mineral.*, **16**, 601–604.

Dunn, P.J., Rouse, R.C., Nelen, J.A. (1985): Hydroxyl-bearing hedyphane from Långban, Sweden. *Geol. För. Stockholm Förhandl.*, **107**, 325–327.

Fleet, M.E., Liu, X., King, P.L. (2004): Accommodation of the carbonate ion in apatite: an FTIR and X-ray structure study of crystals synthesized at 2–4 GPa. *Am. Mineral.*, **89**, 1422–1432.

Friis, H., Balić-Žunić, T., Pekov, I.V., Petersen, O.V. (2004): Kuannersuite-(Ce), $Ba_6Na_2REE_2(PO_4)_6FCl$, a new member of the apatite group, from the Ilímaussaq alkaline complex, south Greenland: description and crystal chemistry. *Can. Mineral.*, **42**, 95–106.

Frost, R.L., Bouzaid, J.M., Palmer, S. (2007): The structure of mimetite, arsenian pyromorphite and hedyphane. A Raman spectroscopic study. *Polyhedron*, **26**, 2964–2970.

Hansen, S. & O'Keeffe, M. (1988): Oriented intergrowth of an antigorite and an arsenate mineral from Långban, Sweden. A natural composite material. *Acta Crystallogr.*, **B44**, 236–242.

Holtstam, D. & Langhof, J. eds. (1999): Långban. The mines, their minerals, geology and explorers. Swedish Museum of Natural History & Raster Förlag, Stockholm.

Holtstam, D. & Mansfeld, J. (2001): Origin of a carbonate-hosted Fe-Mn-(Ba-As-Pb-Sb-W) deposit of Långban-type in Central Sweden. *Mineral. Deposita*, **36**, 641–657.

Hughes, J.M., Cameron, M., Crowley, K.D. (1989): Structural variation in natural F, OH, and Cl apatites. *Am. Mineral.*, **74**, 870–876.

Ivanova, T.I., Frank-Kamenetskaya, O.V., Kol'tsov, A.B., Ugolkov, V.L. (2001): Crystal structure of calcium-deficient carbonated hydroxyapatite. Thermal decomposition. *J. Solid State Chem.*, **160**, 340–349.

Jonsson, E. & Broman, C. (2002): Fluid inclusions in late-stage Pb–Mn–As–Sb mineral assemblages in the Långban deposit, Bergslagen, Sweden. *Can. Mineral.*, **40**, 47–65.

Kabalov, Y.K, Sokolova, E.V., Pekov, I.V. (1997): Crystal structure of belovite-(La). *Phys. Dokl.*, **42**, 344–348.

Krivovichev, S.V. (2012): Derivation of bond-valence parameters for some cation-oxygen pairs on the basis of empirical relationships between r_0 and *b*. *Z. Kristallogr. Cryst. Mater.*, **227**, 575–579.

LeGeros, R.Z., Trautz, O.R., LeGeros, J.P., Klein, E. (1968): Carbonate substitution in the apatite structure. *Bull. Soc. Chim. Fr. (special issue)*, 1712–1718.

Magnusson, N.H. (1930): Långbans malmtrakt. *Sveriges Geologiska Undersökning*, **ser. *Ca*, no. 23**, 1–111.

Mandarino, J.A. (1979): The Gladstone-Dale relationship. Part III. Some general applications. *Can. Mineral.*, **17**, 71–76.

— (1981): The Gladstone-Dale relationship. Part IV. The compatibility concept and its application. *Can. Mineral.*, **19**, 441–450.

Okudera, H. (2013): Relationships among channel typology and atomic displacements in the structures of $Pb_5(BO_4)_3Cl$, with B = P (pyromorphite), V (vanadinite), and As (mimetite). *Am. Mineral.*, **98**, 1573–1579.

Pasero, M., Kampf, A.R., Ferraris, C., Pekov, I.V., Rakovan, J., White, T.J. (2010): Nomenclature of the apatite supergroup minerals. *Eur. J. Mineral.*, **22**, 163–179.

Piotrowski, A., Kahlenberg, V., Fischer, R.X., Lee, X., Parise, J.B. (2002): The crystal structures of cesanite and its synthetic analogues – A comparison. *Am. Mineral.*, **87**, 715–720.

Polya, D.A., Berg, M., Gault, A.G., Takahashi, Y. (2008): Arsenic in groundwater of South-East Asia: with emphasis on Cambodia and Vietnam. *Appl. Geochem.*, **23**, 2968–2976.

Rakovan, J.F. & Pasteris, G.D. (2015): A technological gem: materials, medical, and environmental mineralogy of apatite. *Elements*, **11**, 195–200.

Rouse, R.C., Dunn, P.J., Peacor, D.R. (1984): Hedyphane from Franklin, New Jersey and Långban, Sweden: cation ordering in an arsenate apatite. *Am. Mineral.*, **69**, 920–927.

Sänger, A.T. & Kuhs, W.F. (1992): Structural disorder in hydroxyapatite. *Z. Kristallogr.*, **199**, 123–148.

Schlüter, J., Malcherek, T., Gebhard, G. (2016): Vanackerite, a new lead cadmium arsenate of the apatite supergroup from Tsumeb, Namibia. *N. Jb. Mineral. Abh.*, **193**, 79–86.

Sheldrick, G.M. (2015): Crystal structure refinement with SHELXL. *Acta Crystallogr.*, **C71**, 3–8.

Sjögren, H. (1891): Bidrag till Sveriges mineralogi. *Geol. För. Stockholm. Förhandl.*, **13**, 781–796.

Tazzoli, V. (1983): The crystal structure of cesanite, $Ca_{1+x}Na_{4-x}(SO_4)_3(OH)_x\cdot(1\text{-}x)H_2O$, a sulphate isotypic to apatite. *Mineral. Mag.*, **47**, 59–63.

von Aulock, F.W., Kennedy, B.M., Schipper, C.I., Castro, J.M., Marting, D.E., Oze, C., Watkins, J.M., Wallace, P.J., Puskar, L., Bégué, F., Nichols, A.R.L., Tuffen, H. (2014): Advances in Fourier transform infrared spectroscopy of natural glasses: from sample preparation to data analysis. *Lithos*, **206–207**, 52–64.

Wang, K.L., Zhang, Y., Naab, F.U. (2011): Calibration for IR measurements of OH in apatite. *Am. Mineral.*, **96**, 1392–1397.

White, T.J. & Dong, Z.L. (2003): Structural derivation and crystal chemistry of apatites. *Acta Crystallogr.*, **B59**, 1–16.

Wilson, A.J.C. ed. (1992): International Tables for Crystallography, Volume C: Mathematical, Physical and Chemical Tables. Kluwer Academic, Dordrecht, NL.

Wilson, R.M., Elliott, J.C., Dowker, S.E.P., Smith, R.I. (2004): Rietveld structure refinement of precipitated carbonate apatite using neutron diffraction data. *Biomaterials*, **25**, 2205–2213.

Yi, H., Balan, E., Gervais, C., Segalen, L., Fayon, F., Roche, D., Person, A., Morin, G., Guillaumet, M., Blanchard, M., Lazzeri, M., Babonneau, F. (2013): A carbonate-fluoride defect model for carbonate-rich fluorapatite. *Am. Mineral.*, **98**, 1066–1069.

Received 17 April 2019
Modified version received 29 May 2019
Accepted 30 May 2019